

Gravitational lensing of stars orbiting the Massive Black Hole in the Galactic Center

V. Bozza¹ and L. Mancini²

*Dipartimento di Fisica “E.R. Caianiello”, Università di Salerno, Italy.
Istituto Nazionale di Fisica Nucleare, Sezione di Napoli, Italy.*

ABSTRACT

The existence of a massive black hole in the center of the Milky Way, coinciding with the radio source Sgr A*, is being established on more and more solid ground. In principle, this black hole, acting as a gravitational lens, is able to bend the light emitted by stars moving within its neighborhood, eventually generating secondary images. Extending a previous analysis of the gravitational lensing phenomenology to a new set of 28 stars, whose orbits have been well determined by recent observations, we have calculated all the properties of their secondary images, including time and magnitude of their luminosity peaks and their angular distances from the central black hole. The best lensing candidate is represented by the star S6, since the magnitude of its secondary image at the peak reaches $K = 20.8$, with an angular separation of 0.3 mas from the central black hole, that is just at the borders of the resolution limit in the K band of incoming astronomical instruments.

Subject headings: Gravitational lensing — Black hole physics — Stars: individual (S1, S2, S4, S5, S6, S8, S9, S12, S13, S14, S17, S18, S19, S21, S24, S27, S29, S31, S33, S38, S66, S67, S71, S83, S87, S96, S97) — Galaxy: center

1. Introduction

One of the most fascinating arenas for testing General Relativity in the neighborhood of a real astrophysical black hole is undoubtedly represented by Sgr A*, the massive black hole (MBH) at the center of our Galaxy, whose existence has been now strongly proven by the combination of radio, sub-mm, X-ray, and Near Infrared (NIR) observations. While in the radio domain Sgr A* appears as a steady and motionless compact source (Reid et al. 2007), its X-ray, sub-mm, and NIR counterparts are variable since they exhibit outbursts of energy (*flares*), which typically last for a few hours and occur several times a day (Baganoff et al. 2001, 2003; Genzel et al. 2003;

¹valboz@physics.unisa.it

²lmancini@physics.unisa.it

Ghez et al. 2004; Clénet et al. 2005; Eckart et al. 2006, 2008; Hamaus et al. 2008; Marrone et al. 2008; Yusef-Zadeh et al. 2008). These flares are likely due to energetic events arising very close to the central MBH, on a scale of a few Schwarzschild radii, and they can be interpreted as due to emission from matter in relativistic orbits around Sgr A*. Moreover, by using large class telescopes, such as the ESO Very large Telescope (VLT) and the Keck telescopes, and thanks to the adaptive optics, it has been possible to observe a multitude of stars in the K band (the so-called S-stars) moving in the gravitational potential of the Galactic MBH (Schödel et al. 2003; Ghez et al. 2005; Eisenhauer et al. 2005). The entire system is perfectly described by a single point mass and Newton gravity. Very recently, Gillessen et al. (2008) have been able to determine the orbits of 28 S-stars, resting upon the results of 16 years of monitoring of their motions. In particular, it has been possible to observe the whole orbit of the famous star S2, since it has completed a full revolution around Sgr A*. The value of the Galactic MBH mass, extrapolated from these improved data, is $M = 4.31 \pm 0.36 \times 10^6 M_{\odot}$.

Since the theory of General Relativity predicts that the central MBH can act as a powerful gravitational lens on S-stars, some of them, depending on the knowledge of their orbital parameters, have been the object of careful investigations. The strategy of this study is very clear. In fact, knowing the position of the S-stars in space as a function of time, it is easy to predict the time of their periapse, that is the closest approach to Sgr A*, and look for possible alignments between one of them and the lens, corresponding to the MBH, along the line of sight of an observer on the Earth. In this way, it is possible to foresee at any time where to look for a secondary image, what its apparent magnitude should be, and, thanks to our knowledge of their orbits, easily predict the best time to observe them.

S2 was the first star to be studied as a possible source for gravitational effects due to the central MBH (De Paolis et al. 2003; Bozza & Mancini 2004). The light curve for its secondary image, as well as the first two relativistic images, were calculated in the Schwarzschild black hole hypothesis. The analysis was then enlarged by Bozza & Mancini (2005), who achieved the light curves for the secondary images of five more S-stars. An important fact that emerges from the latter study is that the light curves are peaked around the periapse epoch, but two subpeaks may arise in nearly edge-on orbits, when the source is behind Sgr A* (*standard lensing*) or in front of it (*retrolensing*). In this respect, the star S14 represents an emblematic case.

In the present paper we want to extend the previous analysis of Bozza & Mancini (2005) to the new set of 28 S-stars, provided by Gillessen et al. (2008). We will see that, within these stars, S6 turns out to be a particularly intriguing source for gravitational lensing, since its secondary image is potentially observable by incoming interferometric instruments.

2. Lens Equation and Position of the Images

Our aim is to calculate the position and the luminosity of the secondary images of the 28 S-stars as functions of time, generated by the MBH at the center of our Galaxy. The secondary image appears on the opposite side of the black hole with respect to the source and is thus formed by light rays passing behind the MBH. Defining the deflection angle α as the angle between the asymptotic directions of motion of the light rays, before and after the rendezvous with the black hole, the lens equation is (Ohanian 1987; Bozza & Mancini 2004)

$$\gamma = \alpha(\theta) - \theta - \arcsin\left(\frac{D_{\text{OL}}}{D_{\text{LS}}}\sin\theta\right), \quad (1)$$

where γ is the alignment angle of the source, that is the angle between the line connecting the source to the lens and the optical axis, defined as the line connecting the observer to the lens. The geometry of the lensing configuration is such that γ runs from 0 (perfect alignment) to π (perfect anti-alignment). θ is the impact angle for the light rays as seen from the observer, D_{OL} and D_{LS} are the distances between the observer and the lens, and the lens and the source, respectively. D_{OL} is given by the distance of the Sun to the Galactic center, which is currently estimated to be $R_0 = 8.33 \pm 0.35$ kpc (Gillessen et al. 2008). Following Bozza & Mancini (2005), we obtain D_{LS} and γ as functions of time by an accurate modelling of the Keplerian orbit of the S-stars around the MBH, taking into account the measured values of the orbital parameters. For all the details, the reader is referred to Bozza & Mancini (2005).

As explained in Bozza (2008), the lens equation (1) is the closest to the exact treatment of deflection by a spherically symmetric gravitational field. The relative error in the position of the images committed by using Eq. (1) is at most of the order of $(R_g/D_{\text{LS}})^2$, where $R_g = 2GM/c^2$ is the gravitational radius of the black hole. This number stays lower than 10^{-6} in the worst cases.

The deflection angle is calculated assuming that the black hole is spherically symmetric, thus being described by a Schwarzschild metric. Since the secondary image of an S-star demands a deflection angle in the whole range $[0, \pi]$, we cannot adopt the weak-field or the strong deflection limit approximation, but we have to calculate the exact deflection angle in terms of elliptic integrals (Darwin 1959). Finally, the magnification of a secondary image is given by the general formula (Ohanian 1987; Bozza & Mancini 2004)

$$\mu = \frac{D_{\text{OS}}^2}{D_{\text{LS}}^2} \frac{\sin\theta}{\frac{d\gamma}{d\theta} \sin\gamma}, \quad (2)$$

where D_{OS} is the distance between the observer and the source.

3. Results

In the NIR band, the Sgr A* stellar cluster has been originally observed with the ESO's NTT starting from 1992, then with the Keck from 1995, and with the VLT from 2002. The

good synergy between the adaptive optics and the 8m/10m-class telescopes (Ghez et al. 2001; Schödel et al. 2002) allowed to push the astronomical imaging and the spectroscopy for point sources to a deep sensitivity, that is $K \sim 16\text{--}17$ at an angular resolution of $50\text{--}150$ mas (Eckart et al. 2002). Thanks to these powerful instruments of astronomical investigation, it was possible to monitor the S-stars for more than 16 years and reconstruct for some of them their Keplerian orbits around the Galactic MBH (Gillessen et al. 2008). The orbital parameters of these 28 stars are summarized in table 1.

Following the steps described in Section 2, we have calculated the light curves of the secondary images of the mentioned 28 stars. The main features of these images are presented in table 2, allowing an immediate reading of the results. Besides the values of the minimum magnitude for the secondary images and the epochs at which they peak, we also report the time spent by the secondary images when their luminosity is greater than half of the maximum, the alignment angle and the distance from the MBH of the source stars at the peak, and the maximal angular distance of the secondary images from the apparent shadow of the black hole (whose angular radius is $3\sqrt{3}R_g/2D_{\text{OL}}$ Darwin 1959).

Among all the S-stars analyzed, we concentrate our attention on three particular cases¹: S6, S17, and S27, characterized by a value of the orbit inclination very close to 90° . This feature qualifies them as very appealing candidates for gravitational lensing by the MBH. In Figure 1 we report the light curves for the secondary images of the three mentioned stars (left column) and the alignment angles as functions of time (right column).

S6 – This star is indeed the most interesting one, since its orbit is nearly edge-on ($i = 86.44^\circ$), and its eccentricity brings it quite close to the black hole (up to $4800 R_g$). The best alignment and anti-alignment times are very close to the periapse epoch and are responsible for two subpeaks, see Figure 1a. By examining the Figure 1b, we notice that first we have the alignment peak ($\gamma \sim 0$), and then the anti-alignment peak ($\gamma \sim \pi$). What makes S6 particularly interesting is the high brightness attained by the secondary image. At the best alignment time, that will occur in 2062, the secondary image has a magnitude $K = 20.8$, and the maximal angular distance from the apparent shadow of the MBH is about 0.316 mas, according to the current estimates of the orbital parameters.

S17 – The orbit of this star is nearly edge-on as well ($i = 96.44^\circ$). Yet, contrarily to the previous case, the eccentricity of S17 is very low and the periapse occurs in proximity of one of the nodes. For this reason, the alignment and anti-alignment peaks occur at opposite epochs in the period and neither of them is particularly bright (Figures 1c and 1d).

S27 – From a gravitational-lensing point of view, the inclination of the orbit of this star is the most favorable among all the known S-stars ($i = 92.91^\circ$). Moreover, the eccentricity of the orbit

¹The case of S14 was already examined in Bozza & Mancini (2005). With respect to the estimates presented there, there is no significant change with the new data.

is very close to one. However, the periaapse occurs in correspondence to the anti-alignment epoch (compare Figure 1e with Figure 1f). By reflex, the anti-alignment peak is very tight and hardly visible in Figure 1e because S27 moves very fast at that time. Conversely, the alignment peak is not so bright ($K = 22.4$) as in the case of S6, but anyway better than S14 and S17. It is interesting to note that the angular separation of the secondary image of S27 reaches almost 0.4 mas at the best alignment time, which puts this star in a very good position for possible observations.

4. Discussion

Thanks to the great technological advances earned by the modern big-class telescopes, it has been possible to have access to very remote zones of the Milky Way, like the neighborhood of its center, where the radio source Sgr A* lies. The discovery that most of the detected stars in this region move along tight Keplerian orbits is a strong indication of the existence of a very compact object of more than $4 \times 10^6 M_{\odot}$, currently recognized as a massive black hole, in the geometrical center of the Milky Way. This great disclosure opens an amazing way of escape from the meanders of theoretical speculations and allows us to study gravitational lensing by a black hole on a real case and test General Relativity in its strong field regime. The idea of using the star S2 as a potential source to be lensed by the central MBH, was conceived originally by De Paolis et al. (2003), and then acquired and rigorously developed by Bozza & Mancini (2004, 2005), who considered other S-stars as further possible sources for this phenomenology. In this paper, we extend the previous analysis to a new set of 28 S-stars provided by Gillessen et al. (2008). Whereas most of these stars have undetectable secondary images, there are some cases in which the lensed images have a significant probability of being detected by incoming instruments, as can be deduced from table 2. Among these, S6 represents the best case since its secondary image at the peak reaches $K = 20.8$, with an angular separation of 0.3 mas from the central black hole. Actually, the perspectives for observing such an event are not so far from what the modern technology is developing. In fact, in 2013 the new second-generation VLTI instrument, called GRAVITY, will be scientifically operative at the ESO Paranal observational site (Eisenhauer et al. 2008). This instrument, specifically designed to observe highly relativistic motions of matter close to the event horizon of Sgr A*, will interferometrically combine the NIR light collected by the four-units telescope of the VLT, exploiting all the potential of this extremely powerful ESO observatory. The resolution that will be obtained in the NIR band is ~ 3 mas for objects that can be as faint as $17 < K < 19$. Moreover, in its astrometric mode, GRAVITY will have an accuracy of $10 \mu\text{as}$, allowing to study the motions of celestial objects to within a few times the event horizon size of the Galactic MBH. There are still many years before the secondary images of the best known S-stars will shine again (2047 for S14, 2062 for S6 and S27). Surely, new S-stars will be discovered and followed along their orbits, eventually providing even better candidates for gravitational lensing. In the meanwhile, we have no doubt that the astronomical community will fortify its stock of observational facilities with new advanced instruments, which will be able to catch this extraordinary kind of gravitational lensing events.

Star	a ["']	e	i [$^{\circ}$]	Ω [$^{\circ}$]	ω [$^{\circ}$]	t_P [yr]	T [yr]	K
S1	0.508 \pm 0.028	0.496 \pm 0.028	120.82 \pm 0.46	341.61 \pm 0.51	115.3 \pm 2.5	2000.95 \pm 0.27	132. \pm 11.	14.7
S2	0.123 \pm 0.001	0.88 \pm 0.003	135.25 \pm 0.47	225.39 \pm 0.84	63.56 \pm 0.84	2002.32 \pm 0.01	15.8 \pm 0.11	14.
S4	0.298 \pm 0.019	0.406 \pm 0.022	77.83 \pm 0.32	258.11 \pm 0.3	316.4 \pm 2.9	1974.4 \pm 1.	59.5 \pm 2.6	14.4
S5	0.25 \pm 0.042	0.842 \pm 0.017	143.7 \pm 4.7	109. \pm 10.	236.3 \pm 8.2	1983.6 \pm 2.5	45.7 \pm 6.9	15.2
S6	0.436 \pm 0.153	0.886 \pm 0.026	86.44 \pm 0.59	83.46 \pm 0.69	129.5 \pm 3.1	2063. \pm 21.	105. \pm 34.	15.4
S8	0.411 \pm 0.004	0.824 \pm 0.014	74.01 \pm 0.73	315.9 \pm 0.5	345.2 \pm 1.1	1983.8 \pm 0.4	96.1 \pm 1.6	14.5
S9	0.293 \pm 0.052	0.825 \pm 0.02	81. \pm 0.7	147.58 \pm 0.44	225.2 \pm 2.3	1987.8 \pm 2.1	58. \pm 9.5	15.1
S12	0.308 \pm 0.008	0.9 \pm 0.003	31.61 \pm 0.76	240.4 \pm 4.6	308.8 \pm 3.8	1995.63 \pm 0.03	62.5 \pm 2.3	15.5
S13	0.297 \pm 0.012	0.49 \pm 0.023	25.5 \pm 1.6	73.1 \pm 4.1	248.2 \pm 5.4	2004.9 \pm 0.09	59.2 \pm 3.8	15.8
S14	0.256 \pm 0.01	0.963 \pm 0.006	99.4 \pm 1.	227.74 \pm 0.7	339. \pm 1.6	2000.07 \pm 0.06	47.3 \pm 2.9	15.7
S17	0.311 \pm 0.004	0.364 \pm 0.015	96.44 \pm 0.18	188.06 \pm 0.32	319.45 \pm 3.2	1992. \pm 0.3	63.2 \pm 2.	15.3
S18	0.265 \pm 0.08	0.759 \pm 0.052	116. \pm 2.7	215.2 \pm 3.6	151.7 \pm 2.9	1996. \pm 0.9	50. \pm 16.	16.7
S19	0.798 \pm 0.064	0.844 \pm 0.062	73.58 \pm 0.61	342.9 \pm 1.2	153.3 \pm 3.	2005.1 \pm 0.22	260. \pm 31.	16.
S21	0.213 \pm 0.041	0.784 \pm 0.028	54.8 \pm 2.7	252.7 \pm 4.2	182.6 \pm 8.2	2028.1 \pm 5.5	35.8 \pm 6.9	16.9
S24	1.06 \pm 0.178	0.933 \pm 0.01	106.3 \pm 0.93	4.2 \pm 1.3	291.5 \pm 1.5	2024.9 \pm 5.5	398. \pm 73.	15.6
S27	0.454 \pm 0.078	0.952 \pm 0.006	92.91 \pm 0.73	191.9 \pm 0.92	308.2 \pm 1.8	2059.7 \pm 9.9	112. \pm 18.	15.6
S29	0.397 \pm 0.335	0.916 \pm 0.048	122. \pm 11.	157.2 \pm 2.5	343.3 \pm 5.7	2021. \pm 18.	91. \pm 79.	16.7
S31	0.298 \pm 0.044	0.934 \pm 0.007	153.8 \pm 5.8	103. \pm 11.	314. \pm 10.	2013.8 \pm 2.2	59.4 \pm 9.2	15.7
S33	0.41 \pm 0.088	0.731 \pm 0.039	42.9 \pm 4.5	82.9 \pm 5.9	328.1 \pm 4.5	1967.9 \pm 6.5	96. \pm 21.	16.
S38	0.139 \pm 0.041	0.802 \pm 0.041	166. \pm 22.	286. \pm 68.	203. \pm 68.	2003. \pm 0.2	18.9 \pm 5.8	17.
S66	1.21 \pm 0.126	0.178 \pm 0.039	135.4 \pm 2.6	96.8 \pm 2.9	106. \pm 6.3	1782. \pm 23.	486. \pm 41.	14.8
S67	1.1 \pm 0.102	0.368 \pm 0.041	139.9 \pm 2.3	106. \pm 6.1	215.2 \pm 4.8	1695. \pm 16.	419. \pm 19.	12.1
S71	1.06 \pm 0.765	0.844 \pm 0.075	76.3 \pm 3.6	34.6 \pm 1.5	331.4 \pm 7.1	1646. \pm 251.	399. \pm 283.	16.1
S83	2.79 \pm 0.234	0.657 \pm 0.096	123.8 \pm 1.3	73.6 \pm 2.1	197.2 \pm 3.5	2061. \pm 25.	1700. \pm 205.	13.6
S87	1.26 \pm 0.161	0.423 \pm 0.036	142.7 \pm 4.4	109.9 \pm 2.9	41.5 \pm 3.7	1647. \pm 38.	516. \pm 44.	13.6
S96	1.55 \pm 0.209	0.131 \pm 0.054	126.8 \pm 2.4	115.78 \pm 1.93	231. \pm 9.	1624. \pm 34.	701. \pm 81.	10.
S97	2.19 \pm 0.844	0.302 \pm 0.308	114.6 \pm 5.	107.72 \pm 3.15	38. \pm 52.	2175. \pm 88.	1180. \pm 688.	10.3

Table 1: Orbital Parameters of the S-stars examined in the paper: a is the semimajor axis, e is the eccentricity, i is the inclination of the normal of the orbit with respect to the line of sight, Ω is the position angle of the ascending node, ω is the periaipse anomaly with respect to the ascending node, t_P is the epoch of last/next periaipse, T is the orbital period, K is the apparent magnitude in the K band (data taken from Gillessen et al. 2008).

Star	t_0 [yr]	$t_{1/2}$ [yr]	K_2	θ_2 [μ as]	γ_0 [$^\circ$]	$D_{LS,0}$ [AU]
S1	2130.34	4.9	32.2	54	30.8	2195
S2	2018.15	0.095	26.8	43	45.4	127
S4	2048.94	3.9	28.7	112	12.2	2868
S5	2028.8	2.7	32.9	32	83.6	456
S6	2062.65	0.051	20.8	316	3.56	464
S8	2082.7	1.6	28.3	88	16.2	1335
S9	2041.39	1.9	27.1	144	9.06	1833
S12	2058.38	1.4	32.6	32	88.5	319
S13	2060.3	34	36.4	31	90.8	1571
S14	2047.55	0.073	23.5	136	9.46	230
S17	2008.24	2.1	26.9	196	6.44	2942
S18	2045.15	0.72	30.9	61	26.2	670
S19	2262.63	1.3	29.9	87	16.5	1369
S21	2027.23	1.1	32.3	49	36.5	617
S24	2047.95	44	33.1	81	17.9	6225
S27	2062.08	0.55	22.4	399	2.92	1397
S29	2021.73	0.98	31.6	51	34.1	572
S31	2013.9	0.56	31.7	31	91.2	189
S33	2067.95	9.1	34.9	39	53.7	1637
S38	2021.8	0.71	33.5	32	88.9	242
S66	2254.09	66	36.7	43	45.4	8328
S67	2035.14	116	34.6	40	51.5	9053
S71	2059.51	8.3	31.6	100	13.9	4073
S83	3647.18	129	35.6	50	35.	14435
S87	2185.1	52	35.5	39	53.2	6508
S96	2073.74	131	32.2	48	36.8	14049
S97	2265.5	68	30.9	64	24.6	13897

Table 2: Summary of the main features of the secondary images of the S-stars: t_0 is the epoch of the peak, $t_{1/2}$ is the time spent by the secondary image at a luminosity higher than half the maximum, K_2 is the peak K -band magnitude for the secondary image, θ_2 is the maximal angular distance from the apparent shadow of the black hole, γ_0 is the angle formed by the line connecting the selected star with the central black hole and the optical axis at the time of the peak, and $D_{LS,0}$ is the distance of the S-star from the MBH at this time.

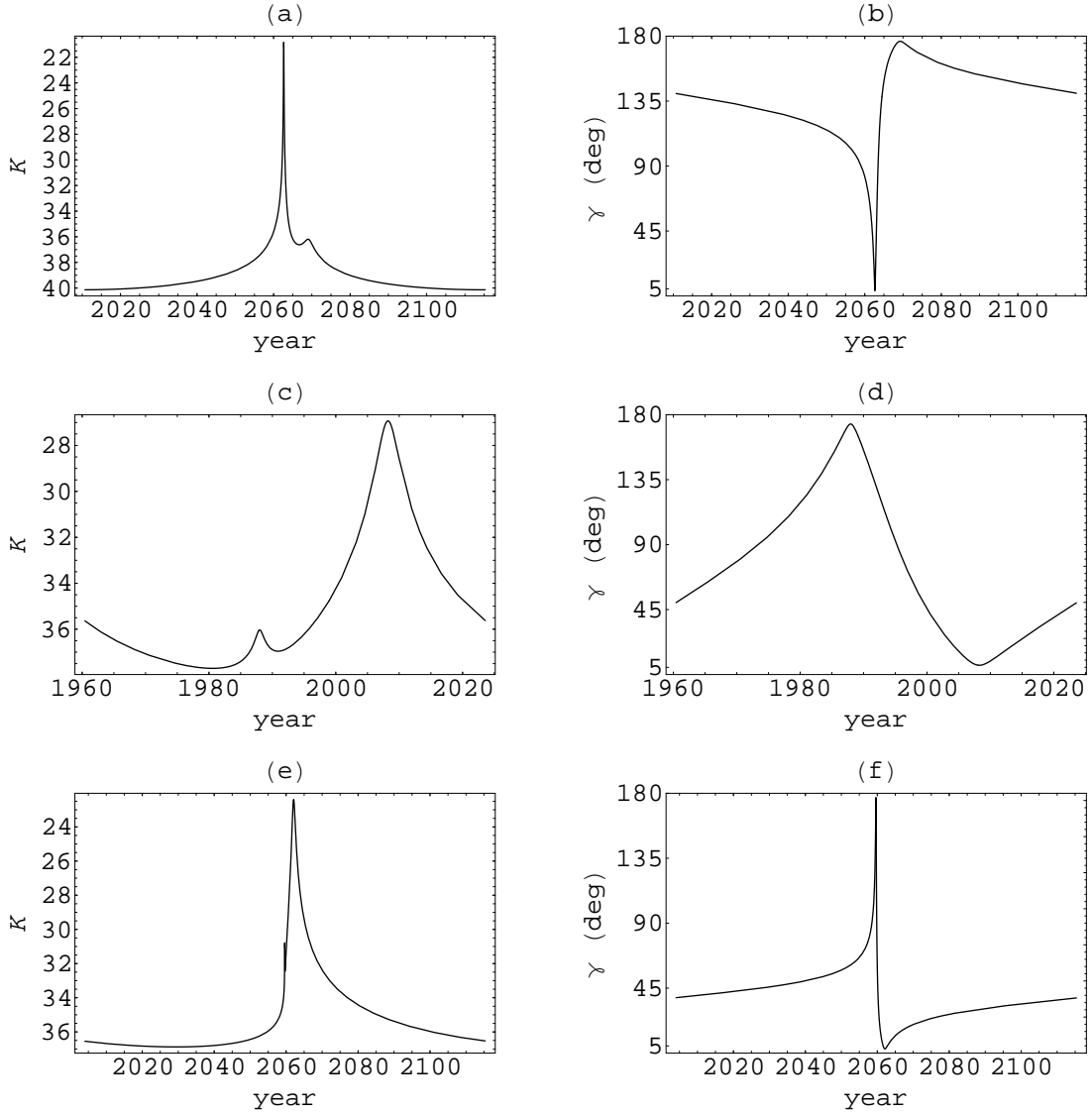


Fig. 1.— Left column: light curves for the secondary images of S6 (a), S17 (c), S27(e). Right column: the alignment angle γ as a function of time for S6 (b), S17 (d), S27(f).

We acknowledge support for this work by MIUR through PRIN 2006 Protocol 2006023491_003, by research funds of Agenzia Spaziale Italiana, by funds of Regione Campania, L.R. n.5/2002, year 2005 (run by Gaetano Scarpetta), and by research funds of Salerno University.

REFERENCES

- Baganoff, F. K., Bautz, M. W., Brandt, W. N., et al. 2001, *Nature*, 413, 45
- Baganoff, F. K., Maeda, Y., Morris, M., et al. 2003, *ApJ*, 591, 891
- Bozza, V. 2008, *Phys. Rev. D*, 78, 103005
- Bozza, V., & Mancini, L. 2004, *ApJ*, 611, 1045
- Bozza, V., & Mancini, L. 2005, *ApJ*, 627, 790
- Clénet, Y., Rouan, D., Gratadour, D., et al. 2005, *A&A*, 439, L9
- Darwin, C. 1959, *Proc. of the Royal Soc. of London*, 249, 180
- De Paolis, F., Geralico, A., Ingresso, G., & Nucita, A. A. 2003, *A&A*, 409, 809
- Eckart, A., Genzel, R., Ott, T., & Schödel, R. 2002, *MNRAS*, 331, 917
- Eckart, A., Baganoff, F. K., Schödel, R. et al. 2006, *A&A*, 450, 535
- Eckart, A., Schödel, R., Garcia-Marin M., et al. 2008, in press with *A&A*, arXiv:0811.2753
- Eisenhauer, F., Genzel, R., Alexander, T., et al. 2005, *ApJ*, 628, 246
- Eisenhauer, F., Perrin, G., Brandner, W., et al. 2008, to appear in the conference proceedings of SPIE Astronomical Instrumentation
- Genzel, R., Schödel, R., Ott, T., et al. 2003, *Nature*, 425, 934
- Ghez, A. M., Morris, M. R., Becklin, E. E., et al. 2001, *ASPC*, 228, 309
- Ghez, A. M., Wright, S. A., Matthews, K., et al. 2004, *ApJ*, 601, L159
- Ghez, A. M., Salim, S., Hornstein, S. D., et al. 2005, *ApJ*, 620, 744
- Gillessen, S., Eisenhauer, F., Trippe, S., et al. 2008, in press with *ApJ*, arXiv:0810.4674
- Hamaus, N., Paumard, T., Müller, T., et al. 2008, in press with *ApJ*, arXiv:0810.4947
- Marrone, D. P., Baganoff, F. K., Morris, M. R., et al. 2008, *ApJ*, 682, 373
- Ohanian, H. C. 1987, *Am. J. Phys.*, 55, 428

- Reid, M. J., Menten, K. M., Trippe, S. et al. 2007, *ApJ*, 659, 378
- Schödel, R., Ott, T., Genzel, R., et al. 2002, *Nature*, 419, 694
- Schödel, R., Ott, T., Genzel, R., et al. 2003, *ApJ*, 596, 1015
- Yusef-Zadeh, F., Wardle, M., Heinke, C., et al. 2008, *ApJ*, 682, 361